PHYSICAL REVIEW B **72**, 121305(R) (2005)

Dynamic polarization tunneling: A spin filtering mechanism

Roberto Romo* and Sergio E. Ulloa
Department of Physics and Astronomy and Nanoscale and Quantum Phenomena Institute, Ohio University, Athens, Ohio 45701, USA
(Received 28 May 2005; published 16 September 2005)

We analyze spin-dependent tunneling in resonant structures using analytic solutions of the time-dependent Schrödinger equation for the spinor components of the problem. These solutions predict a filtering mechanism that occurs in the time domain even for unpolarized injection. The filtering is characterized by dramatic time variations of the spin polarization of tunneling electrons. The time dependence of the transmitted spin critically relies on the interplay between split resonances and the energy at which the electrons are injected into the system. The spin filtering is produced by the tunneling time delays of *different* spin species introduced by the spin-orbit coupling. We derive a simple expression for the dynamic polarization, which shows excellent agreement with the exact numerical solution. The spin dynamical filter should be evident in pulsed injection and probing of charge carriers, and may allow for direct measurement of spin-orbit parameters.

DOI: 10.1103/PhysRevB.72.121305 PACS number(s): 73.40.Gk, 72.25.Mk, 03.65.Xp

Spin-dependent transport in semiconductor heterostructures is an active area of research in the growing field of spintronics. The ability to manipulate electron spins without magnetic fields[1] in nanostructures is of critical importance for the design of spin-injection devices and spin filters.

One of the crucial aspects in the control of spin transport is to understand the effects of the underlying spin-orbit (SO) interaction on the quantum states of the system. In *closed* semiconductor quantum dots, it has been recently shown that both Rashba and Dresselhaus SO Hamiltonians shift the energy levels without breaking their spin degeneracy.[2] These bound states exhibit spin splitting only with the application of an external magnetic field. In contrast, for *open* systems where electron transport is governed by resonant tunneling, a clear splitting of the resonance levels can be accomplished even in the absence of the Zeeman mechanism, provided that the incidence of electrons on a heterojunction plane is tilted rather than strictly perpendicular. The relevance of the nonzero parallel component ($k_\parallel \neq 0$) of the wave vector was noticed early,[3] but its importance in SO effects on tunneling electrons and related quantities is more recent.[4–6] For heterostructures made of semiconductor material with bulk inversion asymmetry, Perel *et al.*[5] have demonstrated that the k^3 Dresselhaus contribution to the effective Hamiltonian of the system couples the spin states and the dynamics of conduction electrons. As shown by Glazov *et al.*[6] this SO coupling leads to a clear spin splitting of the transmission resonances of a double-barrier (DB) system for the different spin species.

The success of experimental techniques based on Kerr and Faraday rotation to measure dynamically the electron spin as it moves in semiconductor heterostructures,[7] strongly motivates theoretical study of time-dependent tunneling phenomena considering SO effects. Even though there is important theoretical work of spin-dependent tunneling,[4–6] the dynamical aspects remain mostly unexplored. It is expected that the spin splitting of the resonance levels has important consequences on the transient regime of tunneling. In the present paper, we analyze the spin-dependent tunneling in DB resonant structures using a quantum-dynamical approach that presents *analytic* solutions of the time-dependent Schrödinger equation for the spinor components of the problem, showing that quantum tunneling produces a natural spin filtering mechanism in the time domain. The spin filtering occurs as a consequence of the different time delays for the tunneling of the two spin species. We find spin-polarized tunneling amplitudes changing with time constants of ~ 1 ps for typical structures. These time scales make the effect suitable for experimental verification and in principle allow for the direct measurements of SO Dresselhaus parameters by optical means.

In the approximation introduced by Perel *et al.*[5] (valid for low kinetic energies), we can write the k^3-Dresselhaus contribution as,

$$\hat{H}_D = \gamma[k_x\hat{\sigma}_x - k_y\hat{\sigma}_y]\partial^2/\partial z^2. \tag{1}$$

The role of other SO terms is small in this low-energy regime, although they exhibit interesting angular and energy dependence.[8,9] It is straightforward to show that the net effect of $\hat{H}_D$ is a renormalization of the effective mass of the electron, so that the effective Hamiltonian for the spinor $S_\pm$ in each semiconductor layer can be written as[6]

$$\hat{H}^\pm = \frac{p^2}{2m_\pm} + \frac{p_\parallel^2}{2m^*} + V(z), \tag{2}$$

where $m_\pm = (1 \pm 2\gamma m^* k_\parallel/\hbar^2)^{-1}$, $S_\pm = (1, \mp e^{i\phi})^T/\sqrt{2}$, the in-plane momentum is $\mathbf{p}_\parallel = p_\parallel(\cos\phi, \sin\phi)$ with $p_\parallel = \hbar k_\parallel$, and $p = -i\hbar\partial/\partial z$. The index $\pm$ in the Hamiltonian and other quantities refers to the rotated spin states $S_\pm$. The potential $V(z)$ consists of a symmetrical DB system that extends along the z axis.

The time-dependent Schrödinger equation

$$i\hbar\frac{\partial}{\partial t}\Psi^\pm = \hat{H}^\pm\Psi^\pm, \tag{3}$$

is solved for $\Psi^\pm = \psi^\pm(z,k,t)\exp[i\mathbf{k}_\parallel\cdot\mathbf{r} - iE_\parallel t/\hbar]$, leading to an independent equation for $\psi^\pm(z,k,t)$. Exact analytic solutions can be obtained for an initial condition of plane waves com-

ing from the left, $\psi_0=\Theta(-z)(e^{ikz}-e^{-ikz})$, where Θ is the Heaviside function.

Since the spinor equation leads in this case to decoupled differential equations for each spinor component $\psi^{\pm}$, one can follow along the procedure for the $\gamma=0$ case[10] and the formal solutions for $z \geqslant L(t>0)$ are

$$\psi^{\pm} = T_k^{\pm} M(y_k^{\pm}) - T_{-k}^{\pm} M(y_{-k}^{\pm}) - \sum_{n=-\infty}^{\infty} T_n M(y_{k_n^{\pm}}^{\pm}). \qquad (4)$$

The quantities $T_q^{\pm}$ refer to transmission amplitudes for $q=-k$, and $+k$, and the factors $T_n^{\pm}=2iku_n^{\pm}(0)u_n^{\pm}(L)\exp(-ik_n^{\pm}L)/[k^2-(k_n^{\pm})^2]$ are given in terms of the resonant eigenfunctions $\{u_n^{\pm}(z)\}$ of the time-independent Schrödinger equation with outgoing boundary conditions. The corresponding complex energy resonant eigenvalues are given by $E_n^{\pm}=\hbar^2(k_n^{\pm})^2/2m^*=\mathcal{E}_n^{\pm}-i\Gamma_n^{\pm}/2$, where $k_n^{\pm}=a_n^{\pm}-ib_n^{\pm}$ ($b_n^{\pm}>0$ and $a_{-n}^{\pm}=-a_n^{\pm}$). The sum runs over the complex poles $\{k_n^{\pm}\}$ distributed in the third and fourth quadrants in the complex k plane. The (Moshinsky) M functions are defined as $M(y_q^{\pm})=\exp[im_{\pm}z^2/2\hbar t]w(iy_q^{\pm})/2$, in terms of the complex error function $w(z)=\exp(-z^2)\mathrm{erfc}(-iz)$, with arguments $y_q^{\pm}=e^{-i\pi/4}(m_{\pm}/2\hbar t)^{1/2}[z-\hbar qt/m_{\pm}]$, where $q=-k,+k,k_n^{\pm},k_{-n}^{\pm}$.

With the above analytic solutions, we can calculate the dynamic spin polarization at any position $z \geqslant L$. At the right edge of the DB system $z=L$, we define

$$\mathcal{P}(E,t) = \frac{|\psi^+(L,E;t)|^2 - |\psi^-(L,E;t)|^2}{|\psi^+(L,E;t)|^2 + |\psi^-(L,E;t)|^2}. \qquad (5)$$

This quantity provides information about the spin state of the tunneling electrons that emerge from the right edge of the system, as a function of both time t and energy of the incident wave, $E=\hbar^2k^2/2m^*$.

Let us consider a DB system with the same parameters as in Glazov *et al.*,[6] appropriate for $Al_xGa_{1-x}Sb$. The solution (4) requires the complex poles $k_n^{\pm}$ of the Green's propagator as input. Figure 1 illustrates the values of the first few poles in the complex k plane for the DB system considered. The splitting of the complex poles (lower inset) is due to the different effective masses produced by the SO interaction, $m_{\pm}$. Here the red (full) dots correspond to "+" spin states and blue (hollow) dots to "−" spin states. Also sketched in the upper inset of the figure is the potential profile with some of its splitting energy resonances (red is for + and blue for −).

Although the series expansion of the formal solution, Eq. (4), involves an infinite number of poles, one can truncate the sum using an appropriate subset of resonances for practical purposes. In our example the incidence energies considered lie in the region of the first resonances; thus the consideration of the first few poles is sufficient to evaluate the solution. The calculation of the dynamic polarization using the first 12 poles (i.e., $n=\pm1,\pm2,\pm3$, for $s=\pm$ states) in Eq. (4) are shown in the contour map of Fig. 2. One can clearly appreciate that there exist regions of intense + polarization (blue) alternating with regions of intense − polarization (yellow), as well as regions with "zero polarization" (green), and intermediate situations.

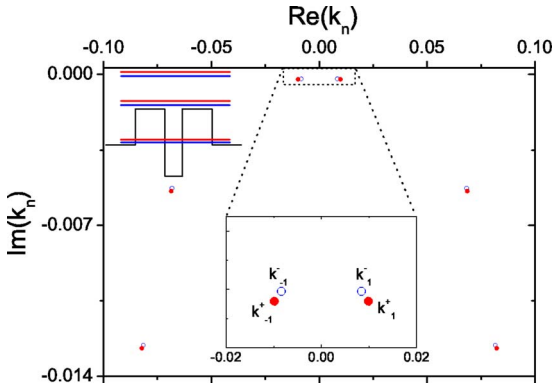

FIG. 1. (Color online) S-matrix poles $k_n^{\pm}$ for a symmetrical DB system for the first few resonances ($n=\pm1,\pm2,\pm3$). The visible splitting of these complex poles is a consequence of the SO interaction; this effect is clearer in the lower inset, where just the four poles with $|n|=1$ are displayed. The potential profile (upper inset) has the parameters: barrier heights $V_0=230$ meV; barrier widths: $b_0=50$ Å; well width: $w_0=30$ Å; and well depth $V_w=-200$ meV. We consider $m^*=0.053m$, $k_{\|}=0.01$ Å^{-1}, and $\gamma=76$ eV Å^3, appropriate for the $Al_xGa_{1-x}Sb$ system.

The role of the resonance doublet $\mathcal{E}_1^{\pm}$ is crucial on the behavior of $\mathcal{P}(E,t)$. Here, the position of these two resonances, whose numerical values are $\mathcal{E}_1^-=5.09$ meV and $\mathcal{E}_1^+=7.02$ meV, are indicated with arrows on the left axis in the figure, and are aligned with the regions of strongest and time-independent polarization. Their corresponding resonance widths are $\Gamma_1^-=0.49$ meV and $\Gamma_1^+=0.64$ meV.

The interesting interplay between the incidence energy and the two resonances seen in Fig. 2 allows one to control the polarization of the transmitted electrons. Depending on the value of E, we will see different behaviors of $\mathcal{P}(E,t)$; note, for example, that when the incidence energy is exactly in between the two resonances, $E=\tilde{\mathcal{E}}\equiv(\mathcal{E}_n^-+\mathcal{E}_n^+)/2=6.05$ meV, the resulting polarization is essentially constant

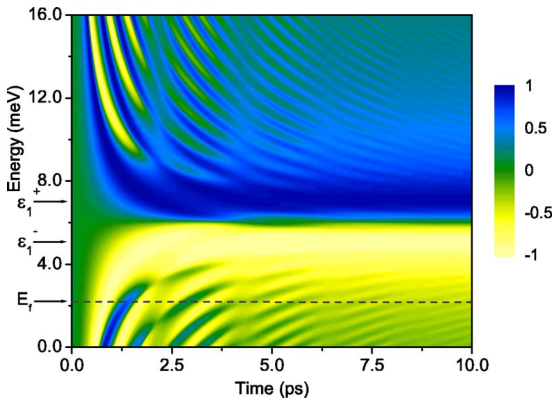

FIG. 2. (Color online) Contour map of the polarization $\mathcal{P}(E,t)$ around the first resonances $\mathcal{E}_1^{\pm}$ of the system in Fig. 1. Blue (dark gray) regions correspond to the strongest positive polarization while yellow (light gray) is for the strongest negative. Note that at certain incidence energies the polarization has dramatic variations with time, as for example going along the cut at $E_f=2.2$ meV (dashed line).

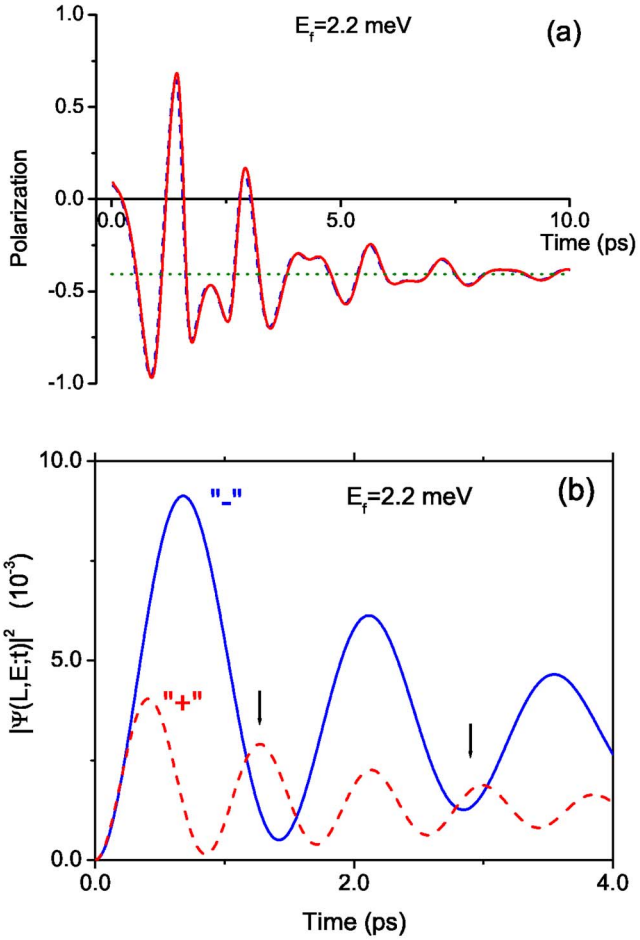

FIG. 3. (Color online) (a) Section of the previous figure at fixed incident energy E_f=2.2 meV. The solid (red) line corresponds to the values of the polarization calculated with the formal solution, Eq. (4). The predicted values by Eq. (7) are included for comparison [dashed lines (blue)]. Both curves coincide almost perfectly and oscillate around the value of the stationary polarization [dotted lines (green)]. (b) Plots of $|\Psi^{\pm}(L,E_f;t)|^2$ vs t for the two spin states. The arrows indicate the intervals where $|\Psi^{+}|^2$ dominates, and the positive polarization in (a).

in time and its value is actually near zero (see the horizontal green stripe in Fig. 2). When the incidence energy matches one of the resonances $\mathcal{E}_1^{\pm}$, the polarization changes smoothly from zero to a constant value (near ± 1, respectively), as these plateaus are their corresponding asymptotes. The most interesting behavior of $\mathcal{P}(E,t)$ occurs for energies slightly below $\mathcal{E}_1^{-}$ (or above $\mathcal{E}_1^{+}$), where dramatic variations of the polarization occur with time; in this case $\mathcal{P}(E,t)$ can adopt positive and negative values at different times.

To illustrate further this variation of $\mathcal{P}(E,t)$, let us make a cut on the contour plot of Fig. 2 at the incidence energy E_f =2.2 meV (see the horizontal dashed line in Fig. 2); the corresponding one-dimensional plot is shown in Fig. 3(a) (red solid line). Notice that, as expected, the time-dependent polarization $\mathcal{P}(E,t)$ tends to the value of the stationary polarization (green dotted line), which is given in terms of the transmission coefficients $T^{\pm}(E)$ by the expression

$$P(E) = \frac{T^{+}(E) - T^{-}(E)}{T^{+}(E) + T^{-}(E)}. \tag{6}$$

However, at intermediate times $\mathcal{P}(E,t)$ oscillates widely with typical times of ~ 1 ps for these parameters (chosen to model a realistic structure).

Note the degree of symmetry exhibited by the polarization map of Fig. 2 with respect to the middle point between the resonances. To clarify this symmetry and to explain the origin of the filtering mechanism, we shall obtain analytic expressions for the square modulus of the spinor components $|\psi^{\pm}|^2$ and hence for the dynamic polarization $\mathcal{P}(E,t)$. Taking into account that the incident energies considered in this study are near the first resonances $\mathcal{E}_1^{\pm}$, and the fact that the poles with different $|n|$ are far apart in Fig. 1, we can use the approximation in which the terms with $|n| \geqslant 2$ are ignored in the solution (keeping only the terms corresponding to the four poles in the inset of this figure). If we now use the analytic properties of the Moshinsky functions and follow an algebraic procedure similar to the derivation of Eq. (11) of Ref. 11, a simple analytic expression for the polarization can be derived, namely

$$\mathcal{P}_a(E,t) = \frac{\mathcal{T}_n^{+}(E,t) - \mathcal{T}_n^{-}(E,t)}{\mathcal{T}_n^{+}(E,t) + \mathcal{T}_n^{-}(E,t)}, \tag{7}$$

$$\mathcal{T}_n^{\pm}(E,t) \equiv T^{\pm}(E)\chi_n^{\pm}(E,t), \tag{8}$$

where the time dependence is contained in the factor

$$\chi_n^{\pm}(E,t) = 1 - 2e^{-t/2\tau_n^{\pm}} \cos \omega_n^{\pm} t + e^{-t/\tau_n^{\pm}}, \tag{9}$$

where $\omega_n^{\pm} = (E - \mathcal{E}_n^{\pm})/\hbar$, and $\tau_n^{\pm} = \hbar/\Gamma_n^{\pm}$ are the lifetimes of the resonant states. This is a simple formula for $\mathcal{P}(E,t)$ since it only requires the value and width of the resonances, as well as the transmission coefficient at each incident energy. Using (7) instead of (5) circumvents the evaluation of the more complicated Moshinsky functions. It is straightforward to see that in the limit $t \to \infty$, we have $\chi_n^{\pm} \to 1, \mathcal{T}_n^{\pm}(E,t) \to T^{\pm}(E)$ and hence $\mathcal{P}_a(E,t) \to P(E)$; that is, the stationary value of the polarization is naturally recovered for long times.

In order to illustrate the accuracy at finite times of Eq. (7), we plot $\mathcal{P}_a(E,t)$ vs t for E_f=2.2 meV (blue dashed line) in Fig. 3(a). We can see that $\mathcal{P}_a$ successfully reproduces the values predicted by the formal solution (5) (red solid line). Notice that $\chi_n^{\pm}(E,t)$ are symmetric functions of E with respect to each of the resonances $\mathcal{E}_n^{\pm}$; this explains the high degree of symmetry observed in the two-dimensional map of the polarization. Equation (7) can also explain other features observed in Fig. 2. Consider, for example, the particular cases of incidence on resonance $E = \mathcal{E}_n^{\pm}$, in which we have $T^{\pm}(\mathcal{E}_n^{\mp}) \ll T^{\pm}(\mathcal{E}_n^{\pm}) = 1$, and hence $\mathcal{P}(\mathcal{E}_n^{\pm}, t) \approx \pm 1$; this is consistent with the two large blue and yellow regions in Fig. 2. Note that, strictly speaking, $\mathcal{P}(\mathcal{E}_n^{\pm}, t)$ does not fully reach the values ± 1 due to the fact that the "tails" $T^{\pm}(\mathcal{E}_n^{\mp})$, although small, are not zero. Another particular case is when the incidence energy matches exactly the middle point between resonances, $E = \tilde{\mathcal{E}}$. In this case, we have $\chi_n^{+}(\tilde{\mathcal{E}}, t) \approx \chi_n^{-}(\tilde{\mathcal{E}}, t)$ and $T_n^{+}(\tilde{\mathcal{E}}, t) \approx T_n^{-}(\tilde{\mathcal{E}}, t)$, which implies that $\mathcal{P}(\tilde{\mathcal{E}}, t) \approx 0$ [in corre-

spondence with the green stripe in the contour map of $\mathcal{P}(E,t)$]. Note again that $\mathcal{P}(\tilde{\mathcal{E}},t)$ is not exactly zero because the width of the resonances, $\Gamma_n^{\pm}$, even when similar, are not the same.

The filtering process in the time domain observed in Figs. 2 and 3(a) can be understood in terms of the time delay between the spinor components arising from the tunneling for a given incident energy. According to Eqs. (8) and (9), $\mathcal{T}_n^{\pm}(E,t)$ are oscillatory functions of time whose frequencies depend on the incident energy E. The only possibility for them to be in phase (i.e., no time delay) is in the particular case $E=\tilde{\mathcal{E}}$. For any other incident energy the "frequencies" $\omega_n^{\pm}$ will be different and both oscillatory patterns will be dephased in time. This is the situation for the energy used in Fig. 3(a) ($E_f=2.2$ meV), and the mentioned dephasing is illustrated in Fig. 3(b), where the values of $\mathcal{T}_n^{\pm}(E,t)$ are plotted separately. In this case, the resonance closer to E is $\mathcal{E}_n^-$, so that we have $T^-(E)>T^+(E)$, and hence $\mathcal{T}_n^-(E,t)$ dominates over $\mathcal{T}_n^+(E,t)$ along the time interval considered, and the predominant polarization is negative. However, the dephasing also produces regions in which the polarization is reversed, corresponding to the intervals in which the $\mathcal{T}_n^{\pm}(E,t)$ curves cross. We can see two of such regions in Fig. 3(b) indicated by arrows, which directly produce the positive peaks of Fig. 3(a).

In summary, we have analyzed spin-dependent tunneling along the transient regime in a resonant structure, finding analytic solutions of the time-dependent Schrödinger equation for the spinor components of the problem. We show that quantum tunneling produces a natural filtering mechanism that occurs in the time domain and is characterized by dramatic variations of the spin polarization of tunneling electrons with time. These strong variations depend critically on the interplay between the energy of the splitting resonances and the energy at which the electrons are injected into the system, which gives rise to different time delays for the tunneling of different spin species. For incident wave packets on resonance, charge accumulation may lead to feedback oscillations[12] that could affect the filtering dynamics; this is not our case, as the incidence is off-resonance and the charge buildup times are much longer than the relevant spin filtering times. Our results indicate that full optical experiments could directly measure the oscillations in polarization and then determine the SO Dresselhaus parameters of the structure.

We thank Mehdi Zarea for useful comments and suggestions. We acknowledge support by the 21st Century Indiana Fund. R. R. thanks the Department of Physics and Astronomy of Ohio University for its hospitality.

*Also at Facultad de Ciencias, Universidad Autónoma de Baja California, Apartado Postal 1880, 22800 Ensenada, Baja California, México. Electronic address: romo@uabc.mx

[1] Y. Kato, R. C. Myers, A. C. Gossard, and D. D. Awschalom, Nature (London) **427**, 50 (2003).

[2] C. F. Destefani, S. E. Ulloa, and G. E. Marques, Phys. Rev. B **69**, 125302 (2004); C. L. Romano, S. E. Ulloa, and P. I. Tamborenea, *ibid.* **71**, 035336 (2005).

[3] T. B. Boykin, Phys. Rev. B **51**, 4289 (1995); V. V. Paranjape, *ibid.* **52**, 10740 (1995).

[4] E. A. de Andrada e Silva, G. C. La Rocca, and F. Bassani, Phys. Rev. B **55**, 16293 (1997); A. Voskoboynikov, S. S. Liu, and C. P. Lee, *ibid.* **58**, 15397 (1998); **59**, 12514 (1999); C. Moysés Araújo, A. Ferreira da Silva, and E. A. de Andrada e Silva, *ibid.* **65**, 235305 (2002).

[5] V. I. Perel, S. A. Tarasenko, I. N. Yassievich, S. D. Ganichev, V. V. Bel'kov, and W. Prettl, Phys. Rev. B **67**, 201304(R) (2003).

[6] M. M. Glazov, P. S. Alekseev, M. A. Odnoblyudov, V. M. Chistyakov, S. A. Tarasenko, and I. N. Yassievich, Phys. Rev. B **71**, 155313 (2005).

[7] I. Malajovich, J. J. Berry, N. Samarth, and D. D. Awschalom, Nature (London) **411**, 770 (2001); I. Malajovich, J. M. Kikkawa, D. D. Awschalom, J. J. Berry, and N. Samarth, Phys. Rev. Lett. **84**, 1015 (2000); J. M. Kikkawa and D. D. Awschalom, Nature (London) **397**, 139 (1999).

[8] G. E. Marques, A. C. R. Bittencourt, C. F. Destefani, and S. E. Ulloa, Phys. Rev. B **72**, 045313 (2005).

[9] E. I. Rashba and A. L. Efros, Phys. Rev. Lett. **91**, 126405 (2003).

[10] G. García-Calderón and J. Villavicencio, Phys. Rev. A **64**, 012107 (2001); G. García-Calderón and A. Rubio, *ibid.* **55**, 3361 (1997).

[11] R. Romo, Phys. Rev. B **66**, 245311 (2002).

[12] C. Presilla, G. Jona-Lasinio, and F. Capasso, Phys. Rev. B **43**, R5200 (1991).